

DEVELOPING ARTIFICIAL MUCUS HYDROGEL THAT MIMICS CYSTIC FIBROSIS AIRWAY
MUCUS

by
Xiaoxin Wang

A thesis submitted to Johns Hopkins University in conformity with the requirements for the
degree of Master of Science in Engineering.

Baltimore, Maryland

May 2019

© 2019 Xiaoxin Wang
All Rights Reserved

Abstract

Cystic fibrosis (CF) is one of the most common genetic lung diseases caused by a mutation of the chloride regulator in airway cells, which leads to dysregulation of ion transport and airway dehydration. As a result, airway mucus in CF patients (i.e. CF sputum) is highly viscoelastic and hard to be cleared by physiological mucus clearance mechanism, thereby promoting chronic infection and inflammation. Previously, bacteria cell growth and neutrophil-mediated bacterial cell killing were studied with mucus solution prepared with different concentration of mucin which is the major macromolecular component of airway mucus. However, mucus solution does not recapitulate airway mucus on the account of failure to form physiological gel-like structures relevant to behaviors of bacteria and neutrophils. Thus, to investigate the effect of microstructure of mucus on these behaviors on the cellular and molecular levels, we developed artificial irreversible and bio-reducible mucus hydrogel with well-defined pore sizes and similar biochemical contents comparable to CF airway mucus, by chemically crosslinking porcine gastric mucin (PGM). Since CF patients are often treated with mucus-altering agents (i.e. mucolytics) to reduce the viscoelasticity of mucus, we not only evaluated the microstructure of artificial mucus hydrogel *per se* but also examined the mucolytic-mediated microstructural changes using multiple particle tracking method. The results here show that the microstructure and mucolytic-mediated microstructure changes of artificial bio-reducible mucus hydrogels are comparable to what were observed in CF sputum. And we also confirmed that bulk rheology of bio-reducible artificial mucus is comparable to that of CF sputum. In addition, mucolytic-mediated changes in bulk rheology properties of the mucus hydrogel and CF sputum were virtually identical. Furthermore, we investigated the biochemical properties of bio-reducible mucus hydrogel (i.e. mucin and,

cysteines content), and lastly, the ability of bacteria to grow in artificial bio-reducible mucus hydrogel. These results show that the artificial bio-reducible mucus hydrogel is a promising model to investigate the effect of mucus microstructure on mucosal pathogenesis and innate immunity in CF airways.

Advisor: Dr. Jung Soo Suk

Reader: Dr. Stavroula Sofou

Contents

Acknowledgments.....	viii
Introduction.....	1
1.1 The structure and function of airway mucus.....	1
1.2 Cystic Fibrosis.....	2
1.3 The formation of pathologic mucus	2
1.4 Recent progress in CF mucus study	3
1.5 Motivation.....	4
Materials and Methods.....	6
2.1 Develop artificial mucus hydrogel model	6
2.2 Develop mucus-inert nanoparticle (MIP).....	7
2.3 Particle characterization and stability test.....	8
2.4 human Specimens.....	8
2.5 Characterize artificial mucus hydrogel and CF sputum with and without mucolytics treatment.....	8
2.6 Multiple particles tracking analysis.....	9
2.7 Particle-tracking microrheology analysis.....	10
2.8 Examine the rheology of bio-reducible mucus hydrogel	11

2.9 Examine the disulfide bonds in PGM solution, bio-reducible mucus hydrogel and CF sputum	11
2.10 Examine the mucin concentration of bio-reducible artificial mucus hydrogel and CF sputum	12
2.11 Bacteria Culture in Hydrogel	12
2.12 Statistical Analysis	13
Results and Discussion	14
3.1 Developing mucus-penetrating nanoparticles	14
3.2 Microstructural properties of irreversible artificial hydrogels	16
3.3 Microstructure properties of artificial bio-reducible hydrogels	18
3.4 Biochemical properties of bio-reducible mucus hydrogel	21
3.5 Bacteria growth in bio-reducible mucus hydrogel	22
Conclusion	24
Future work	26
Reference	27
Curriculum Vitae	30

List of Figures

Figure 1. Stability of nanoparticles in mucin solution.....	15
Figure 2. Microstructure analysis of irreversible cross-linked mucin hydrogel and patients' sputum sample.	16
Figure 3. The effect of mucolytic (TCEP) on microstructure of irreversible crosslinked mucin hydrogel and patients' sputum sample.....	17
Figure 4. Microstructure analysis of bio-reducible cross-linked mucin hydrogel and patients' sputum sample.	18
Figure 5. Microstructure analysis of bio-reducible cross-linked mucin hydrogel.	19
Figure 6. Characterization of microstructure change in bio-reducible cross-linked mucin-based hydrogels.....	20
Figure 7. Bulk rheology of bio-reducible mucus hydrogel with and without mucolytic treatment.	21
Figure 8. Biochemical measurements of Bio-reducible cross-linked mucin hydrogel and CF patients' sample.	22
Figure 9. Growth of <i>P. aeruginosa</i> strain in different mucin-based models.	23

List of Tables

Table 1. Physiochemical properties of nanoparticles	15
---	----

Acknowledgments

Firstly, I'd like to thank my advisor Jung Soo Suk, who helped me a lot on my project, and my mentor Siddharth Shenoy, who give me instruction and help me to improve my critical, creative and independent thinking skills.

I'd also like to thank: Dr. Daiqin Chen, Dr. Kai Zhang, who helped me with polymer conjugation; Aditya Josyula, Dr. Yumin Oh and Dr. Kevin DeLong, who helped me with bacteria culture; and all people in my lab, who gave me kind help. I'd like to also thank Dr. Natalie West for providing clinical CF samples, and Paula Mister for providing the bacterial cultures.

Also, I would like to acknowledge that these research efforts were made possible by support from the Cystic Fibrosis Foundation.

Last but not least, I want to thank my friends who always accompany with me whenever I'm happy or upset, and I also want to thank my parents who are always support me on every decision I made.

Introduction

1.1 The structure and function of airway mucus

Mucus provides a physiological barrier to environmental toxins and pathogens and is one of the first lines of innate immune defense in the conducting airway epithelium [1]–[4]. Normal mucus clearance is mediated by a two-phase liquid system that interfaces with beating cilia [5]. The upper phase is a mucus layer, which is a polymeric network that has bulk viscoelastic physical characteristics despite being made up of ~97% water. Thus, mucus is a polymeric gel with both fluid and solid properties, such as soft, elastic and viscous [3], [6]–[9]. The composition of normal mucus are 97% water and 3% solids (mucins, non-mucin proteins, salts, lipids and cellular debris). Mucins are exceedingly large glycoproteins, the monomer of which is typically 10-40 MDa in size and 0.2-0.6 μm and linked together by disulfide bonds. The multimers are like long flexible strings densely coated with O-linked N-acetyl galactosamine and N-linked sulfate-bearing glycans, which are negatively charged [7], [10]–[15]. These glycosylated and highly hydrophilic regions are separated by hydrophobic regions that fold into hydrophobic globules which stabilized by multiple internal cysteines-rich domains [7], [10]–[15]. Five of the secreted mucins have terminal cysteine rich domains that can form disulfide bonds resulting in polymers that impart the properties of a gel. Two of these polymers, MUC5AC and MUC5B, are highly expressed in the airways [7], [9], [15]. They form the mucus gel both by network entanglement and by noncovalent calcium-dependent cross-linking of adjacent polymers [6], [13]. Since the mucin chain can bind to large amounts of water, this can act as a liquid reservoir for periciliary layer [16]. The hydration of mucus significantly affects the viscosity and elasticity of mucus, which in turn determines the

ciliary action and the clearance effect of mucus [3], [6], [8], [13], [16], [17]. However, excessive secretion of mucin or maladjustment of surface fluid volume hinders clearance of mucus and increased mucus elasticity [3], [6], [8].

1.2 Cystic Fibrosis

Cystic fibrosis (CF) is one of the most common inherited chronic disease that affects nearly 30,000 individuals in United States [18]. A hallmark of CF is chronic respiratory infection, which may start very early in the life of these patients. And much of morbidity and mortality associated with CF is related to the pulmonary system, primarily the upper and lower airways and ultimately leading to premature death in 90% of patients [19], since CF is caused by mutations in the CF transmembrane conductance regulator (CFTR) gene, which encodes the main anion channel expressed in the epithelium [20]. The most accepted hypothesis is that the mutation of CFTR causes a defect in CFTR proteins, and thus, a lack of transport of chloride and accompanying water across the airway epithelium. Then, excessive sodium reabsorption lead to dehydration of airway surface fluid and impaired mucociliary clearance. The resulting increased viscosity of mucus result in the inability of clearing secretions, which leads to chronic infection, inflammation and irreparable mucus clearance [5], [18], [21], [22]. Even patients that are treated with antibiotics and mucolytics that modify properties of mucus still suffer from irreparable lung damage.

1.3 The formation of pathologic mucus

In patients with cystic fibrosis, MUC 1, 2, 5AC and 5B are translated and MUC5AC and MUC5B products have been demonstrated to be the major components in airway mucins [23]. The characteristics of CF mucus are neutrophil infiltration, high concentrations of neutrophil-derived

DNA and actin filaments [9], [24]; infection with organisms such as *Pseudomonas aeruginosa*, *Staphylococcus aureus*, and aspergillus species, often form biofilms at the epithelial-cell surface.

The dehydrated, highly entangled polymeric macromolecule that forms a gel matrix with a reduced pore size from about 500 nm to about 150 nm [3]. The reduction in pore size lead to immobilize the microorganisms in the mucus gel, thereby improving the formation of biofilms and inhibiting the movement of neutrophils that prevents clearing the infection [25]. The effects of these processes are manifested (a) radiographically as bronchiectasis, (b) pathologically as neutrophilic inflammation, airway fibrosis, (c) increased numbers of mucin-secreting cells, especially in the submucosal glands, (d) clinically as cough, purulent sputum, recurrent lung infections, and (e) rapid loss of lung function [26]–[28].

1.4 Recent progress in CF mucus study

To investigate the effect of airway surface liquid (ASL) hyperabsorption on bacteria biofilm formation, Matsui, etc. used normal (2.5% solids wt/wt) and CF-liked (8%) concentrations of mucus which obtained from well differentiated human airway cultures as model to mimic the interaction of inhaled bacteria with a central feature of the CF lung. By investigating bacteria microcolony development, they found that the concentrated mucus (8%) generates a unique environment in which bacteria are confined spatially so that the capacity of bacteria to leave the site by their normal means of motility is restrained [29]. They also investigated the ability of neutrophil capture and killing bacteria by similar model. Furthermore, they found that in CF-like concentrated mucus (6.5%) harvested from *in vitro* airway epithelial cells, the ability of neutrophil capture and killing bacteria are suppressed [30]. However, they mainly focused on the bulk property of mucus as in mucus concentration (e.g. % solids contents).

In our previous study, it was proved that the microrheological and microstructural properties of human mucus secretions can be assessed by monitoring the diffusion rates of muco-inert nanoparticle (MIP) probes, also referred to as mucus-penetrating particles (MPP) in our prior studies [8], [31]–[33]. MIP with diameters smaller than mucus mesh spacings are capable of efficiently penetrating sputum since dense surface coatings with polyethylene glycol (PEG) render the particle surface muco-inert. MIP transport in mucus is primarily hindered by physical obstruction imposed by the mucus mesh structure rather than adhesive interactions [33], [34]. Duncan GA, et al., correlated patient-specific sputum microstructural properties and solids content with clinical status, FEV₁ (i.e. the maximal amount of air you can forcefully exhale in one second). And they found that percent solids content which did not significantly correlate well with FEV₁, however, the microstructures of mucus Log₁₀ (median MSD_{1s}) were positively and significantly correlated with measured FEV₁ [21].

1.5 Motivation

Mucus hypersecretion and airway dehydration lead to pulmonary exacerbation associated with polymicrobial infection both virus and bacteria, which means that a CF patient at particular point of time may be infected with a number of different organisms. And the phenotype of bacteria like *Pseudomonas aeruginosa* may also change from non-mucoid to mucoid state when patients have been infected for a prolonged period of time [19]. Thus, due to the complex microenvironment in CF airway mucus, it is hard for researchers to understand the behavior of bacteria and the distribution of inflammatory cells based on effect of microstructure. Thus, in order to get better understanding of bacteria behavior and inflammatory cell distribution, it is necessary to develop an artificial mucus hydrogel to mimic CF patients' sputum not only from solids content but also from microstructure features.

Thus, in this study, we developed both irreversible and bio-reducible artificial mucus hydrogel to mimic CF airway mucus by crosslinking mucin from porcine stomach with different crosslinkers. We further assessed the microstructure of artificial mucus hydrogel with different crosslinking density, evaluated the mucolytics-mediated microstructure changes, and bulk rheology changes of artificial mucus hydrogel compared with that of CF airway mucus. We also examined the biochemical components such as the mucin content and disulfide bonds (e.g. cysteine concentration) in artificial hydrogel. We compared these components with those found in CF airway mucus. These results will establish a promising model to investigate the effect of mucus microstructure on pathogenesis and inflammatory cells transport.

Materials and Methods

2.1 Develop artificial mucus hydrogel model

For non-bio-reducible artificial hydrogel model, pig gastric mucin (PGM) solutions were prepared by dissolving PGM (Porcine gastric mucin, Sigma-Aldrich) with buffer solution containing 154mM NaCl, 3mM CaCl₂, and 15mM NaH₂PO₄ at pH 7.4 and were rapidly mixed for 2 hours using a magnetic stir plate to achieve concentration of 10% (w/v). MW 1000 SC-PEG-SC (Biochempeg Scientific Inc.) which contain NHS ester at two arms at varying final concentrations were added dropwise to PGM solutions to achieve a final concentration of 5% (w/v). The solution was mixed by pipetted several times. And the mixed solution was incubated overnight in the shaker at 37°C, 225 RPM to allow cross-linking to occur. The cross-linked mucus hydrogel was subsequently collected by centrifugation at 17, 000 g for 1 hour. The supernatant was removed, and the pellet was then flash frozen in liquid N₂ and lyophilized overnight. The lyophilized, cross-linked mucus hydrogels were reconstituted to the final overall solids content of 5% in the original buffer solution and then the hydrogels swelled for 24 hours before being used.

For bio-reducible artificial hydrogel model, hydrogels mainly composed of PGM were prepared by addition of MW 2000 OPSS-PEG-OPSS (Laysan Bio, Lnc.). PGM solution with concentration of 10%, 20% 30% and 40% were prepared with same way. The PGM solutions with different concentrations were treated with Dithiothreitol (DTT) (Sigma-Aldrich). The molar ratio of disulfide bonds in PGM solution and DTT is 1:2. The solutions were mixed by vortexing at the highest speed for 1 min. The mixed solutions were incubated at 37°C water bath for 2 hours to break the disulfide bonds. OPSS-PEG-OPSS was dissolved with original buffer solution and then mixed into PGM solution. The molar ratio of OPSS-PEG-OPSS and thiol group is 2:1. After mixed

by pipetted several times and quickly vortexed, the mixed solutions were incubated in 37°C shaker with shaking at 225 RPM for 48 hours to allow cross-linking to occur. The pellets were subsequently collected by centrifugation at 17,000 g for 1 hour and the supernatant was removed. The pellet was then flash frozen in liquid N₂ and lyophilized overnight. The lyophilized, cross-linked mucus hydrogels were reconstituted to the final overall solids content of 5% in the original buffer solution and then the hydrogels swelled for 24 hours before used.

2.2 Develop mucus-inert nanoparticle (MIP)

Fluorescent, carboxylate-modified polystyrene spheres (PS-COOH) with 100 nm diameter (Molecular Probes) were coated by covalently with 5 KDa methoxy-PEG-amine (Creative PEGWorks) using carbodiimide coupling chemistry. The PS-COOH particles were sonicated for 10 min prior to aliquoting. The aliquoted particles were diluted 4-fold in ultrapure water and then were sonicated for 7 min. PEG 5K-NH₂ were added 2-fold excess to the particle suspension. After mixing the suspension solution and dissolving the PEG-NH₂, N-hydroxysulfosuccinimide sodium salt (sulfo-NHS, Sigma-Aldrich) was added and quickly dissolved by vortexing. The mixed solution was diluted 5 times by 200mM borate buffer, pH 8.2. 1-ethyl-3-(3-dimethylaminopropyl) carbodiimide hydrochloride (EDC, Invitrogen) was added immediately and mixed by vortexing. The mixed solution was incubated at room temperature and mixed for at least 12 hours. After incubation, the particle solution was dialyzed in ultrapure water for 24 hours by using the Spectra/Por Dialysis membrane MWCO: 100KD (Biotech CE Tubing) to remove byproducts. The dialyzed particle solution was collected and lyophilized overnight. The particle pellet was resuspended to achieve solid content 2%. The modified particles were stored in 4°C fridge before using.

2.3 Particle characterization and stability test

Particle characterization: PS particles and PSPEG particles were diluted in 10 mM NaCl at pH 7.4, and then added in to pre-washed disposable folded capillary cells (Malvern) for zeta potential and UV-transparent disposable cuvettes (Sarstedt, Int.) for hydrodynamic diameter and polydispersity index (PDI). The zeta potential and size were tested using Zetasizer Nano ZS90.

Particle stability test: PGM solution with different concentration was made with the original buffer solution. The PEG coated particles PSPEG and non-coated particles PS were diluted 1000 times with PGM solution. The solutions were mixed by sonicated 5 min. Then 150 μ L mixed particle solution were added in the UV-transparent disposable cuvettes (Sarstedt, Int.). the size of each particles was measured at different time points by using Zetasizer Nano ZS90 (Malvern Instruments), at 137° scattering angle.

2.4 Human specimens

Spontaneously expectorated CF sputum samples were collected from patients at the adult CF clinic at Johns Hopkins University. And the microstructures of CF sputum samples were characterized within 24 hours, since after 24 hours the microstructures of sputum samples would change significantly because of degradation of mucins. And the rest of CF sputum samples used for biochemical properties analysis were stored in -80°C freezers.

2.5 Characterize artificial mucus hydrogel and CF sputum with and without mucolytics treatment

Ten microliter aliquots of hydrogels were dispensed in custom microscopy slides using positive-displacement pipette (Gilson, Inc.). Next, 0.5 μ L of pre-mixed PSPEG and PS particles with concentration of 0.002% and 0.0002% were dispersed gently in the hydrogel and CF sputum

samples. Also, to test the effect of mucolytic on hydrogel and CF sputum samples, 0.5 μL TCEP or 0.5 μL NAC were added into hydrogel to achieve 10-20 mM final concentration of mucolytics. The slides were sealed with a small coverslip to prevent evaporation and the slides were incubated for 30 min to 1 hour and avoiding the light. Samples were imaged at room temperature using an Axio Observer inverted epifluorescence microscope and $\times 100/1.46$ NA oil-immersion objective with image resolution of 25 nm/pixel (Zeiss). To avoid edge effects due to the presence of glass coverslips, images were taken centrally within the sample approximately 2 μm away from the bottom coverslip. Videos were recorded at a frame rate of 15 Hz for 300 frames, using an EM-CCD camera (Evolve 512; Photometrics). For each sample, 3–5 videos were collected.

2.6 Multiple particles tracking analysis

Motions of nanoparticles were captured at 15 frames per second (i.e. exposure time of 67 ms) for 20 seconds and MetaMorph software (Molecular Devices, San Jose, CA) were used. The time-averaged mean squared displacement (MSD) values are averaged squared distances travelled by individual particles at a given time interval (i.e. timescale in seconds) and thus are directly proportional to particle diffusion rates. The analysis was performed using automated software written in MATLAB (Mathworks), based on a previously developed algorithm. Briefly, the x and y positions of nanoparticle centers were determined based on an intensity threshold. Trajectories of particles were constructed by connecting particle centers of all images and obtaining the moving distance between each frame. The time-averaged mean squared displacement $[\text{MSD}(\tau)]$ can be calculated for each particle trajectory: $\langle \Delta r^2(\tau) \rangle = \langle [x(t + \tau) - x(t)]^2 + [y(t + \tau) - y(t)]^2 \rangle$, where τ is the time lag between frames. The median values were determined based on measured MSD for individual particle. Also, we have found previously that when MSD measured at $\tau = 1\text{ s}$ (e.g.

MSD_{τ=1s}), the static error does not cause significant effects on calculated MSD values. Based on this, Log₁₀(median MSD_{τ=1s}) was used as our primary readout for evaluating hydrogel pore size.

2.7 Particle-tracking microrheology analysis

The viscoelastic properties of hydrogels can be determined using the generalized Stokes-Einstein relation, which has been successfully used in prior studies of CF sputum, which relates the viscoelastic spectrum $[G(s)]$ to the Laplace transform of $\langle \Delta r^2(\tau) \rangle$, $\langle \Delta r^2(s) \rangle$, with the equation $G(s) = 2k_B T / [\pi a s \langle \Delta r^2(s) \rangle]$ by assuming that the local viscoelastic modulus around a sphere is the same as the macroscopic viscoelastic modulus, where $k_B T$ is thermal energy, a is particle radius, and s is the complex Laplace frequency, $s = i \omega$, in which i is a complex number and ω is frequency. Based on this, the complex modulus can be calculated as $G^*(\omega) = G'(\omega) + G''(i\omega)$ defined by storage modulus and loss modulus which given by $G_r(t)$. The elastic modulus per blob is in an order of $k_B T$, where k_B is the Boltzmann constant and T is the absolute temperature. In polymer gels, the elastic blob is considered to be equal to the geometric blob (the size of the average distance between the crosslinkers or branch points); the polymer chains between crosslinkers are the elastically effective chains. The net elastic modulus (G') of the gel is written as the product of number density of elastic blob (ρ_{el}), the elastic modulus per blob is: $G' = \rho_{el} k_B T$. By assuming a cubic lattice for simplicity, the size of elastic blob is given as: $\xi_{el} = \rho_{el}^{-1/3}$. Thus, the pore size of the sputum hydrogel (ξ) can be estimated based on measured G' as $\xi \approx (k_B T / G')^{1/3}$ [35]–[38]. The microviscosity and pore size values were determined from individual PSPEG trajectories rather than based on ensemble average MSD, given the heterogeneous nature of PSPEG transport in CF sputum samples.

2.8 Examine the rheology of bio-reducible mucus hydrogel

Rheological measures were derived from a MCR 302 Rheometer (Anton Paar Germany GmbH) with 8 mm roughened flat plate geometry set at a gap height of 150 microns. An aliquot of 25 microliters of mucin hydrogel was placed between plates with the following procedures. For TCEP experiments, the gel was pre-incubated with 10-20 mM TCEP for 30 minutes before recording the data using Rheoplus V3.6 software (Anton Paar). An amplitude sweep was performed on each hydrogel to determine an appropriate strain rate. The G' and G'' values were derived from the linear viscoelastic regime of the frequency sweep between 0.1 to 10 rad/s at 5-10% strain at 25°C.

2.9 Examine the disulfide bonds in PGM solution, bio-reducible mucus hydrogel and CF sputum

CF sputum, PGM solution with different concentrations and bio-reducible mucus hydrogel with different pore size were papered using the original buffer and then diluted 10 times in 8M Guanidine Hydrochloride solution (Sigma-Aldrich). The diluted solutions were vortexed until became clear and homogeneous. The clear solutions were added 0.5M iodoacetamide (Sigma-Aldrich) such that the final concentration is 10% (v/v) and incubation at room temperature for 1 hour. 1M DTT was added such that the final concentration is 10% (v/v) and then the solutions were incubated at 37°C water bath for 2 hours. All small molecules were removed using premade zeba spin desalting columns. The column's bottom closure was removed, and the cap was loosed. The columns were placed in a 1.5-2.0 mL collection tube, and then centrifuged at 1500 g for 1 minute to remove storage solution. The columns were placed in a new tube. Sample was slowly added to the center if the compacted resin bed. The columns with sample were centrifuged at 1500 g for 2 minutes to collect desalted sample. The serial dilutions of standard from 5mM L-cysteine (Sigma-Aldrich) were made. The 70 μ L volume of 10 times diluted samples and standards were

added to plate. 70 μ L of 2mM bromobimane (Sigma-Aldrich) were added to well and mixed. The plate was incubated at room temperature for 15 minutes and then read values by fluorescence (395 excitation/ 490 emission) with auto scale option checked. All fluorometric measurements were performed using a microplate reader (BioTek Synergy Mx) [39].

2.10 Examine the mucin concentration of bio-reducible artificial mucus hydrogel and CF sputum

The hydrogel sample was diluted with buffer solution containing 0.01M Na₂HPO₄ and 0.04% NaN₃ at pH 7.4. Several dilutions of Mucin from bovine submaxillary glands (BSM) were made with filtered borate-phosphate buffer containing 0.3M borate, 0.3M phosphate dibasic at pH 8.0. 0.5M Cyanoacetamide (Sigma-Aldrich) were made fresh. 0.1 mL Mucin solutions and sputum samples were mixed with 0.25 mL 0.5M Cyanoacetamide and 0.5 mL borate-phosphate buffer. The mixed solutions were incubated in oven for 3 hours at 100°C. The solutions were cooled by putting vials on ice for 15 min. Then solutions were aliquot into plate and read values by fluorescence (331 excitation/ 380 emission) with auto scale option checked [40], [41].

2.11 Bacteria Culture in Hydrogel

To measure the bacteria growth in mucin from porcine stomach (PGM) and artificial bio-reducible hydrogel, 1 μ l droplets (\approx 2000 CFU) *P. aeruginosa* were deposited on 15 μ l of PGM (5% solids) and bio-reducible hydrogel (5% solids) of very MSD values in chambers. Before depositing *P. aeruginosa* in broth, 5% PGM and hydrogel, part of the stock bacteria suspension was collected, diluted with PBS, and plated on tryptic soy agar plates after serial dilution to test the starting number of *P. aeruginosa*. After that at 24, 48 h later, bacteria in PGM and hydrogel were collected, diluted with PBS containing 10mM DTT, and plated on tryptic soy plates after serial dilution. The

CFU (Colony-Forming Unit) of *P. aeruginosa* at different time point were counted after overnight incubation [29].

2.12 Statistical Analysis

Statistical analysis and graphs were performed in Prism (GraphPad, San Diego, CA). Two sample comparisons were made using two-tailed, paired t-tests. All P values are two-sided and $P < 0.05$ was considered significant.

Results and Discussion

3.1 Developing mucus-penetrating nanoparticles

In our prior studies, we have shown that nanoparticles (NPs) with carboxylate and hydrophobic polystyrene (PSCOOH) cores are immobilized by mucus via muco-adhesion by hydrophobic and electrostatic interactions regardless of particle size [31], [42]. But polystyrene particles with hydrophilic coatings of high-density PEG are able to move through the pores in entangled mucin network by steric hindrance and thus, do not perturb biophysical properties of airway mucus. Therefore, these pegylated PSCOOH probes can measure the pores in the microstructure of mucus. We can infer about the size of the pores since the diffusion of particles is primarily blocked by steric interactions [43]. If size of NP < pore size, then particles are mobile, and if size of NP > pore size, then particles are immobilized. Our previous studies have established that 100 nm PSPEG particles are able to probe and be sensitive to the microstructure of mucus from patients with cystic fibrosis (CF) [21], [32], [43].

Furthermore, 100 nm PSPEG particles were developed and characterized along with PS counterparts by using dynamic light scattering and laser Doppler anemometry in this study. As shown in **Table 1**, we found that while the hydrodynamic diameters, polydispersity indices, and $\text{Log}_{10}(\text{Median MSD}_{t=1s})$ in H₂O of size-matched PSPEG and PSCOOH were comparable, the ζ -potentials (i.e. an indicative of particles surface charge) of PSPEG were near neutral charge unlike highly negatively charged PSCOOH.

Table 1. Physiochemical properties of nanoparticles

Particle Type	ζ -potential ^{α} (mV)	Hydrodynamic Diameter ^{β} (nm)	Polydispersity Index ^{β}	Log (Median MSD t=1s) in H2O
100 nm PSCOOH	-35.7 ± 1.8	87.9 ± 3.8	0.1 ± 0.01	0.76
100 nm PSPEG	-4.1 ± 0.2	98.0 ± 6.9	0.1 ± 0.01	0.79

^{α} Measured in 10 mM NaCl at pH 7.4.

^{β} Hydrodynamic diameter and polydispersity index measured by dynamic light scattering

In our previous study, we have tested the stability of PSPEG particles in physiological lung fluid, and the results show that PSPEG particles are stable in physiological fluid. Since we made bio-reducible mucus hydrogel based on PGM solution, we also evaluated the stability of PSPEG particles in pig gastric mucin (PGM) solution. As shown in **Figure 1**, while both PSCOOH and PSPEG retained their particle diameters at first 4 hours in 0.1 mg/mL PGM solution, only PSPEG particles were capable of retaining their stability within 6 hours of incubation at room temperature.

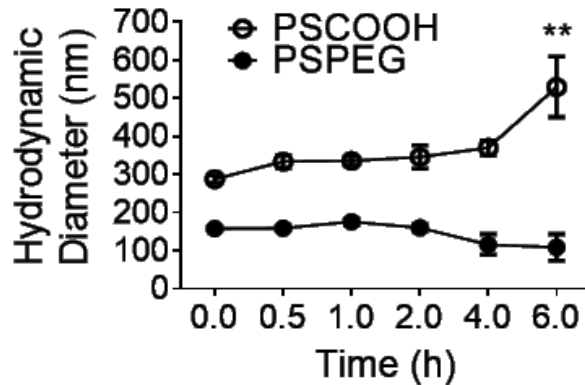


Figure 1. Stability of nanoparticles in mucin solution. Compared with PS particles which aggregated in mucin solution, PSPEG particles were stable in 0.1% mucin content after 6 hours of incubation at 25°C. (** $p < 0.01$, two-tailed, paired t-test, $n = 3$)

3.2 Microstructural properties of irreversible artificial hydrogels

Irreversible mucin-based hydrogels were developed by crosslinking mucin fibers (PGM) using 1000 Da SC-PEG-SC, which contain NHS ester groups at the side of two arms that react with amine groups in the mucin gel solution. After formulation (see Methods), the resulting bulk viscoelastic properties of the model mucus gel were confirmed qualitatively by an inversion test (**Figure 2A**). As evidenced by 100-nm PSPEG transport rates in mucin-based hydrogels at a fixed solids content of 5%, increasing the SC-PEG-SC concentration led to an increase in crosslinking density of mucin-based hydrogel, thereby reducing mesh pore size, as shown in **Figure 2B**. We next compared the Log_{10} (Median MSD $\tau=1s$) of 100 nm PSPEG of irreversible hydrogel with that of CF sputum samples. We found that the Log_{10} (Median MSD $\tau=1s$) varied among CF patients and median values of CF sputum are comparable with that of artificial irreversible hydrogels (**Figure 2C**).

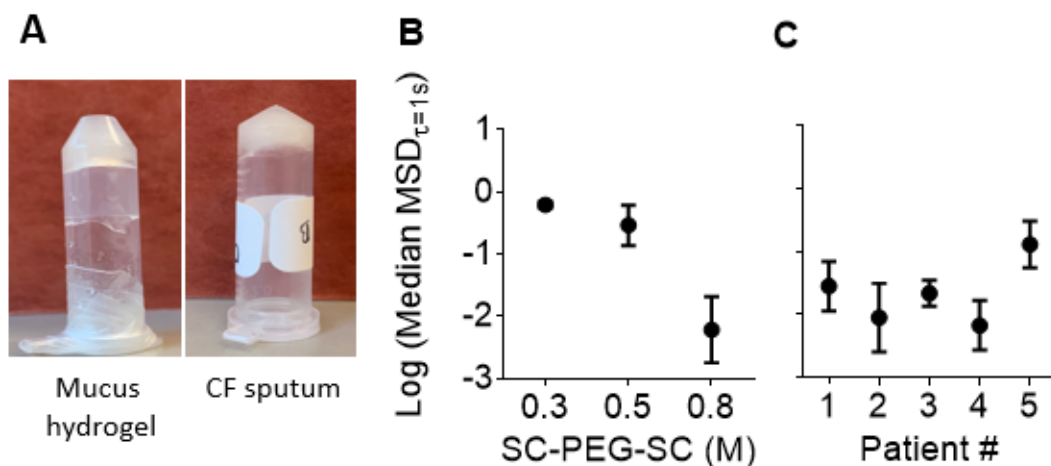


Figure 2. Microstructure analysis of irreversible cross-linked mucin hydrogel and patients' sputum sample. (A) Inversion test of a sample in an Eppendorf tube showing bulk viscoelastic properties of permanent cross-linked mucin-based hydrogel (containing 5% solids) and a CF sputum sample (right) at room temperature. Log_{10} (Median MSD $\tau=1s$) measured in (B) Irreversible mucin hydrogel ($n = 3$ replicates) by varying final concentrations of crosslinker and (C) patients' sputum samples ($n = 3$ replicates per patient sample). Values listed as mean \pm SEM.

We also investigated the impact of mucus-altering agent on microstructure of the artificial irreversible hydrogels, since our previous studies have shown the microstructural changes of CF sputum samples occur with mucolytic agents. Thus, in our study, we treated artificial irreversible hydrogel and CF sputum samples with TCEP and compared the mucolytic-mediated microstructure changes of them. As shown in **Figure 3A & B**, while TCEP was able to alter the microstructure of CF sputum mucus, this agent was unable to change the microstructure of artificial irreversible mucus hydrogel. Due to the limited change in $\text{Log}_{10}(\text{Median MSD}_{\tau=1s})$ of artificial irreversible hydrogel by the mucus-altering agent, we turned to creating a bio-reducible mucus hydrogel to closely mimic reduction of CF sputum.

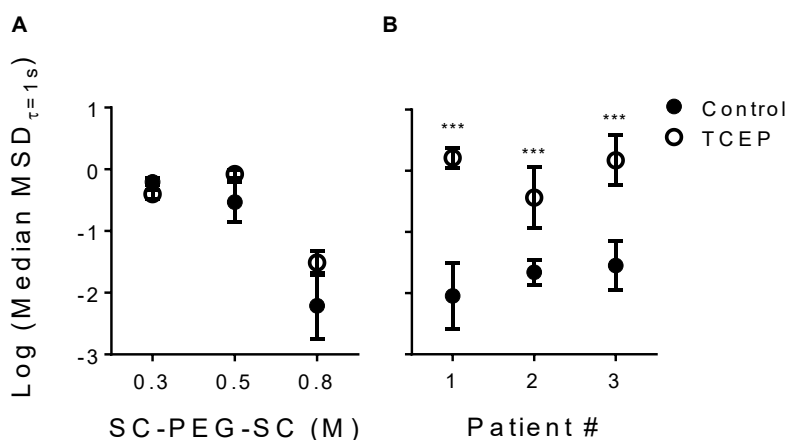


Figure 3. The effect of mucolytic (TCEP) on microstructure of irreversible crosslinked mucin hydrogel and patients' sputum sample. (A) $\text{Log}_{10}(\text{Median MSD}_{\tau=1s})$ measured in irreversible mucin hydrogel with and without treatment with TCEP ($n = 3$ replicates) under varying final concentrations of cross-linker. (B) $\text{Log}_{10}(\text{Median MSD}_{\tau=1s})$ measured in patients' sputum sample with and without treatment with TCEP (***) $p < 0.001$, two-tailed paired t-test, $n = 3$ replicates per patient sample). Values displayed as mean \pm SEM.

3.3 Microstructure properties of artificial bio-reducible hydrogels

Considering that the mechanism of mucus-altering agents such as NAC and TCEP is breaking disulfide bonds in cysteines domain, and in turn reducing the size of mucin polymer chain, we chose another crosslinker to crosslink mucin with disulfide bridges, which is 1000 Da OPSS-PEG-OPSS, contains pyridyl disulfide ethyl at edge of two arms enabling to directly synthesize disulfide bonds via disulfide thiol interchange, and the byproduct Pyridine-2-thione is very stable. The artificial bio-reducible mucus hydrogel with increasing cross-linking density engineered by controlling the initial concentration of PGM solution, as shown in **Figure 4A**. We next compared the $\text{Log}_{10}(\text{Median MSD}_{\tau=1s})$ of 100 nm PSPEG of bio-reducible hydrogel with that of CF sputum samples. We found that the $\text{Log}_{10}(\text{Median MSD}_{\tau=1s})$ varied among CF patients' sputum are comparable with that of artificial bio-reducible hydrogels (**Figure 4B**). The resulting bulk viscoelastic properties of the model mucus gel were confirmed qualitatively by an inversion test (**Figure 4C**).

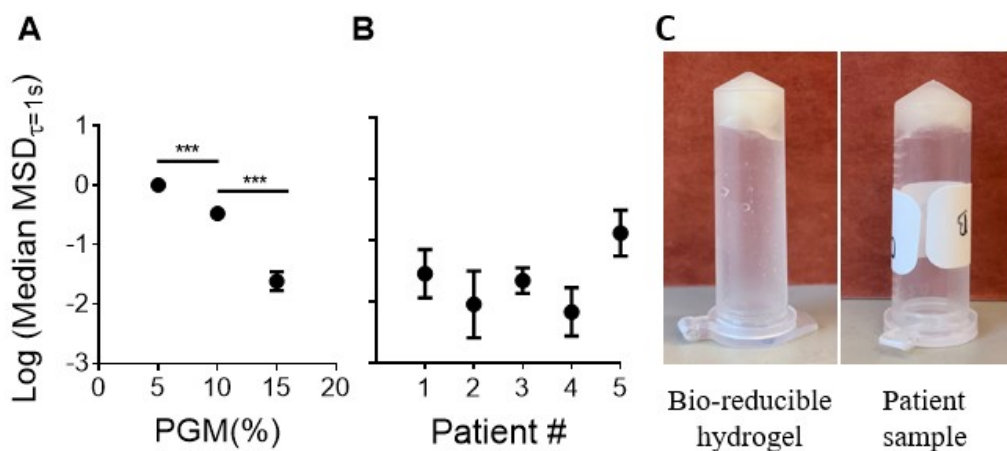


Figure 4. Microstructure analysis of bio-reducible cross-linked mucin hydrogel and patients' sputum sample. $\text{Log}_{10}(\text{Median MSD}_{\tau=1s})$ measured in (A) bio-reducible mucin hydrogel varied by final concentration of PGM (w/v %) and (B) patients' sputum samples. Values represented as mean \pm SEM. (C) Inversion test showing bulk viscoelastic properties of bio-reducible cross-linked

mucin-based hydrogel (containing 5% solids) and a CF sputum sample (right). (** $p < 0.001$, $n = 3$)

The mean pore size was also determined for artificial bio-reducible mucus hydrogel (**Figure 5**) from MSD values (**Figure 4A**). The impact of mucus-altering agent on microstructure of developed artificial bio-reducible hydrogels was also evaluated. We treated artificial bio-reducible hydrogel and CF sputum samples with two different mucolytics TCEP and NAC. As shown in **Figure 6A & B**, NAC was able to alter the microstructure of both bio-reducible hydrogel and CF sputum mucus with $\text{Log}_{10}(\text{Median MSD } \tau=1s)$ around -1. However, no significant difference of microstructure changes was found in artificial bio-reducible hydrogel and CF mucus with $\text{Log}_{10}(\text{Median MSD } \tau=1s)$ around 0 and -2. And as shown in **Figure 6C & D**, TCEP was able to alter the microstructure of artificial bio-reducible hydrogel and CF sputum mucus with $\text{Log}_{10}(\text{Median MSD } \tau=1s)$ around -1 and -2. Based on these observations, TCEP appears more effective compared to NAC on reducing the viscoelasticity of mucus.

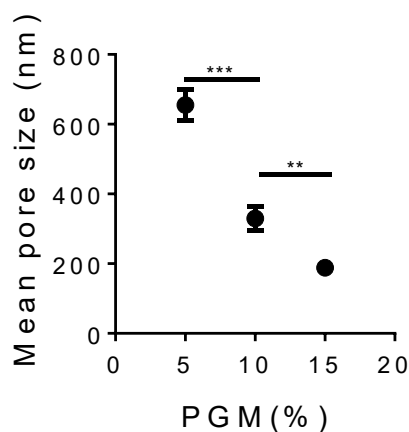


Figure 5. Microstructure analysis of bio-reducible cross-linked mucin hydrogel. Mean pore size measured in bio-reducible mucin hydrogel based on an obstruction scaling model[35], [44]. (** $p < 0.01$, *** $p < 0.001$, $n = 3$)

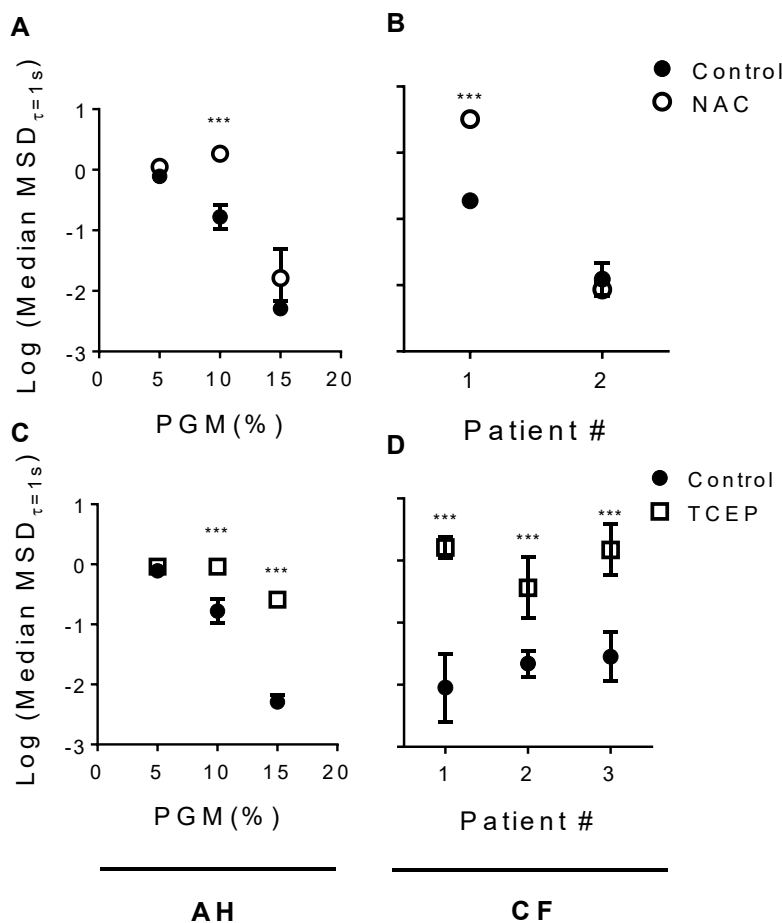


Figure 6. Characterization of microstructure change in bio-reducible cross-linked mucin-based hydrogels. AH: artificial bio-reducible mucus hydrogel (A) $\text{Log}_{10}(\text{Median MSD}_{\tau=1s})$ measured in bio-reducible mucin hydrogel with and without treatment with NAC. (B) $\text{Log}_{10}(\text{Median MSD}_{\tau=1s})$ measured in patients' samples with and without treatment with NAC. (C) $\text{Log}_{10}(\text{Median MSD}_{\tau=1s})$ measured in bio-reducible mucin hydrogel with and without treatment with TCEP. (D) $\text{Log}_{10}(\text{Median MSD}_{\tau=1s})$ measured in patients' samples with and without treatment with TCEP. (***) $p < 0.001$, two-tailed t-test, $n = 3$)

Also, according to these data, the mucolytic-mediated microstructural changes of artificial bio-reducible mucus hydrogel is comparable to what is observed in CF sputum. Of note, bulk rheology of bio-reducible mucus hydrogel with and without mucolytic treatment were also investigated (Figure 7A & B). We can see in figure A and B the Bulk elastic and viscous moduli significantly reduced upon mucolytic TCEP treatment in bio-reducible hydrogel with 180nm pore size, which

further confirmed the mucolytics responses of bio-reducible hydrogel in bulk size. And by comparing the storage and loss moduli with dash lines in figure which are literature values of CF sputum [45], we found that the bulk rheology of bio-reducible artificial mucus hydrogel is comparable to rheology of CF sputum.

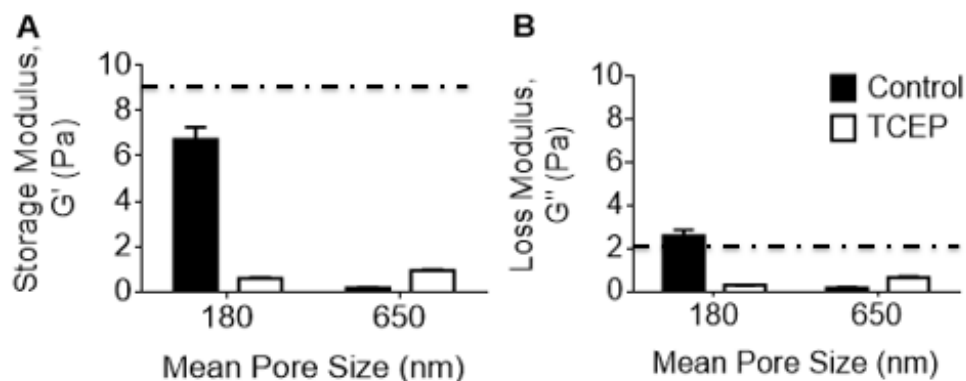


Figure 7. Bulk rheology of bio-reducible mucus hydrogel with and without mucolytic treatment. (A) Storage modulus of bio-reducible mucin hydrogel (B) Loss modulus of bio-reducible mucin hydrogel. Values estimated as mean \pm SEM from frequency sweep between 0.1 to 1 rad/s along linear viscoelastic (LVE) regime with 5-10% strain. The dash lines are literature values of CF sputum's storage and loss moduli [45]. Values shown as mean \pm SEM along LVE.

3.4 Biochemical properties of bio-reducible mucus hydrogel

As mentioned above the solids content of bio-reducible hydrogel is 5%. In order to ensure that other biochemical components (mucin and cysteine contents) in bio-reducible hydrogel is comparable to those in CF patients' sputum samples. The mucin and cysteine content in bio-reducible hydrogel and CF sputum were quantitatively measured. The range of mucin content in bio-reducible hydrogel is from 15 mg/mL to 25 mg/mL (**Figure 8A**), which is comparable with the range of mucin content in CF sputum have shown in **Figure 8B** (10 mg/mL–25 mg/mL).

Similarly, the cysteine content in bio-reducible hydrogel is in the range of mucin content in CF sputum. (Figure 8C & D).

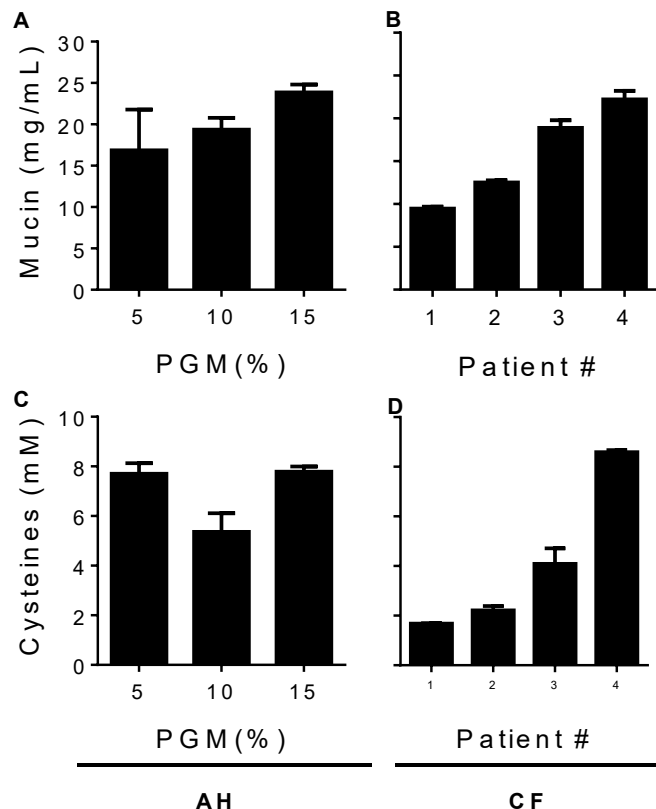


Figure 8. Biochemical measurements of Bio-reducible cross-linked mucin hydrogel and CF patients' sample. AH: artificial bio-reducible mucin hydrogel (A) Mucin concentration in bio-reducible mucin hydrogel with different pore size. (B) Mucin concentration in CF patients' sputum samples. (C) Cysteines concentration in bio-reducible mucin hydrogel with different pore size. (D) Cysteines concentration in CF patients' sputum samples. (A) and (B) A fluorescent assay using cyanoacetamide (CNA) shows that the concentration of mucin in artificial bio-reducible hydrogel is in the ranges of that in CF sputum (n = 3). (C) and (D) A fluorescent assay using dithiothreitol (DTT) and monobromobimane (mBBr) shows that the number of cysteines of artificial bio-reducible hydrogel is in the ranges of that of CF sputum (n = 3).

3.5 Bacteria growth in bio-reducible mucus hydrogel

Based on previous studies, a vexing problem in CF pathogenesis has been to explain the high prevalence of *Pseudomonas aeruginosa* biofilms in CF airways and *P. aeruginosa* is the major pathogen infecting the CF lung. Thus, *P. aeruginosa* has been chosen in our study on whether

developed bio-reducible hydrogels are suitable for bacteria growth. *P. aeruginosa* grew and within 24 h reached the stationary phase at 10^8 cfu/chamber for broth and 5% PGM solution (**Figure 9A**) served as control group. *P. aeruginosa* grew in bio-reducible hydrogel with 330 nm and 180 nm mean pore size reached the stationary phase at 10^8 cfu/chamber within 24 hours. *P. aeruginosa* grew in bio-reducible hydrogel with 650 nm mean pore size reached the stationary phase at 10^6 cfu/chamber within 24 hours and achieve 10^7 cfu/chamber within 48 hours (**Figure 9B**). These two figures have shown that bio-reducible artificial mucus hydrogel does not undermine the intrinsic ability of bacterial cells to grow.

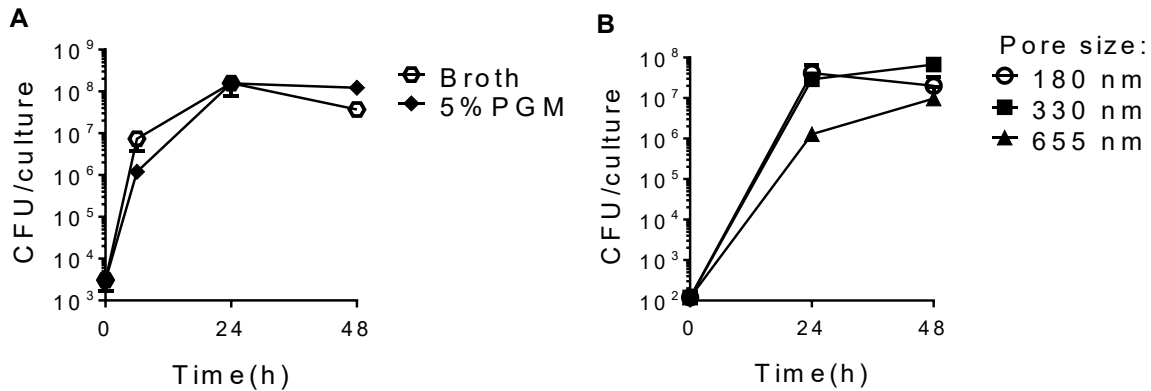


Figure 9. Growth of *P. aeruginosa* strain in different mucin-based models. (A) Bacterial growth curve in broth and 5% PGM. Approximately 2000 *P. aeruginosa* were deposited in broth and 5% PGM solution. Number of bacteria was counted at 0, 6, 24, 48 h intervals; n=3. (B) Growth curve of bacteria in bio-reducible mucin hydrogel with different pore size. Bacteria were counted at 24 and 48 h time points, n=2.

Conclusion

On account of the complexity of microenvironment in CF airway mucus, it is hard for researchers to get deep understanding of behavior of bacteria and distribution of inflammatory cells. Although in previous study, mucus with high solids content from well-differentiated human airway cultures are used as model to investigate the microcolony development and neutrophil migration, the poor correlation between solids content and clinical status, FEV₁ indicated that this model based solely on solids content potentially is lacking to to mimic CF airway mucus. We hypothesize that microstructural properties significantly correlate with clinical outcome in previous study.

Thus, we have developed an artificial mucus hydrogel with defined pore size and solids content with PGM and different crosslinker to try to mimic CF airway mucus. By crosslinking PGM solution with SC-PEG-SC, we synthesized irreversible mucus hydrogel. Although the microstructures of irreversible mucus hydrogel are comparable with that of CF sputum, the mucolytic-mediated microstructural changes of irreversible hydrogel were not as significant as observed in CF sputum. After that, we developed bio-reducible artificial mucus hydrogel by crosslinking PGM with OPSS-PEG-OPSS. We demonstrated that the microstructure of bio-reducible mucus hydrogel is comparable to that of CF airway mucus, and its mucolytic-mediated microstructural changes are same with what observed in CF sputum. We also evaluated the bulk rheology and rheology changes after mucolytic treatment, the result confirmed that the rheology of bio-reducible mucus hydrogel is comparable to that of CF sputum. We compared the mucin and cysteines content in bio-reducible hydrogel with those in CF sputum. These results have shown that the contents of mucin and cysteines in bio-reducible hydrogel were in the range of mucin and cysteines in CF sputum. Thus, based on these evaluations, bio-reducible artificial mucus hydrogel

has been validated and can serve as a model to mimic airway CF mucus to help us understand the behavior of bacteria colonization and inflammatory cells migration.

Future work

After we evaluated the bio-reducible artificial hydrogel comprehensively, we can further use this model to understand the behavior of bacteria and distribution of inflammatory cells. Although Matsui, H et al. group have previously studied bacteria distribution in mucus with different solids content, we still know little about the relationship between microstructure of mucus and bacteria colony distribution. By investigating the microcolony development of bacteria in bio-reducible hydrogel we could understand the effect of microstructure on bacterial microcolony development. And to explore whether the microstructure of hydrogel will affect neutrophil velocity and whether neutrophil would be trapped in hydrogel with small pore size, we will examine the neutrophil migration in bio-reducible hydrogel. We can further investigate the ability of neutrophil to capture bacteria in bio-reducible hydrogels with different pore size to examine the effect of microstructure of mucus on neutrophil-bacteria capture.

Also, since there are some other diseases relating to mucus in other part of body, by altering the type of mucin to crosslink and controlling the ratio of crosslinker, we could develop an artificial mucus hydrogel model to mimic mucus in other part of our body, for example, gastrointestinal tract mucus. The artificial mucus hydrogel model can help us understand pathologies of different mucoviscid diseases.

Reference

- [1] M. A. Hollingsworth and B. J. Swanson, “Mucins in cancer: Protection and control of the cell surface,” *Nat. Rev. Cancer*, vol. 4, no. 1, pp. 45–60, 2004.
- [2] S. K. Linden, P. Sutton, N. G. Karlsson, V. Korolik, and M. A. McGuckin, “Mucins in the mucosal barrier to infection,” *Mucosal Immunol.*, vol. 1, no. 3, pp. 183–197, 2008.
- [3] R. A. Cone, “Barrier properties of mucus,” *Adv. Drug Deliv. Rev.*, vol. 61, no. 2, pp. 75–85, 2009.
- [4] M. R. Knowles *et al.*, “Ion composition of airway surface liquid of patients with cystic fibrosis as compared with normal and disease-control subjects,” *J. Clin. Invest.*, vol. 100, no. 10, pp. 2588–2595, 1997.
- [5] R. C. Boucher, “Airway Surface Dehydration in Cystic Fibrosis: Pathogenesis and Therapy,” *Annu. Rev. Med.*, vol. 58, no. 1, pp. 157–170, 2007.
- [6] D. J. Thornton, “From Mucins to Mucus: Toward a More Coherent Understanding of This Essential Barrier,” *Proc. Am. Thorac. Soc.*, vol. 1, no. 1, pp. 54–61, 2004.
- [7] M. C. Rose and J. A. Voynow, “Respiratory Tract Mucin Genes and Mucin Glycoproteins in Health and Disease,” *Physiol. Rev.*, vol. 86, no. 1, pp. 245–278, 2006.
- [8] S. K. Lai, Y.-Y. Wang, D. Wirtz, and J. Hanes, “Micro- and macrorheology of mucus,” *Adv. Drug Deliv. Rev.*, vol. 61, no. 2, pp. 86–100, 2009.
- [9] J. V. Fahy and B. F. Dickey, “Airway Mucus Function and Dysfunction,” *N. Engl. J. Med.*, vol. 363, no. 23, pp. 2233–2247, 2010.
- [10] G. Lamblin *et al.*, “The Carbohydrate Diversity of Human Respiratory Mucins: A Protection of the Underlying Mucosa?,” *Am. Rev. Respir. Dis.*, vol. 144, no. 3_pt_2, pp. S19–S24, 2013.
- [11] P. Georgiades, P. D. A. Pudney, D. J. Thornton, and T. A. Waigh, “Particle tracking microrheology of purified gastrointestinal mucins,” *Biopolymers*, vol. 101, no. 4, pp. 366–377, 2014.
- [12] S. KIRKHAM, J. K. SHEEHAN, D. KNIGHT, P. S. RICHARDSON, and D. J. THORNTON, “Heterogeneity of airways mucus: variations in the amounts and glycoforms of the major oligomeric mucins MUC5AC and MUC5B,” *Biochem. J.*, vol. 361, no. 3, pp. 537–546, 2015.
- [13] M. Kesimer *et al.*, “Tracheobronchial air-liquid interface cell culture: a model for innate mucosal defense of the upper airways?,” *Am. J. Physiol. Cell. Mol. Physiol.*, vol. 296, no. 1, pp. L92–L100, 2008.
- [14] C. L. Hatstrup and S. J. Gendler, “Structure and Function of the Cell Surface (Tethered)

- Mucins,” *Annu. Rev. Physiol.*, vol. 70, no. 1, pp. 431–457, 2007.
- [15] D. J. Thornton, K. Rousseau, and M. A. McGuckin, “Structure and Function of the Polymeric Mucins in Airways Mucus,” *Annu. Rev. Physiol.*, vol. 70, no. 1, pp. 459–486, 2007.
- [16] M. R. Knowles and R. C. Boucher, “Innate defenses in the lung,” *J. Clin. Invest.*, vol. 109, no. 5, pp. 571–577, 2002.
- [17] S. M. Kreda, C. W. Davis, and M. Callaghan Rose, “CFTR, Mucins and Mucus Obstruction in Cystic Fibrosis,” *Semin. Respir. Crit. Care Med.*, vol. 30, no. 05, pp. 587–595, 2009.
- [18] T. S. Cohen and A. Prince, “Cystic fibrosis- a mucosal immunodeficiency syndrome NATURE 2012,” vol. 18, no. 4, pp. 509–519, 2013.
- [19] C. H. Goss and J. L. Burns, “Exacerbations in cystic fibrosis: 1: Epidemiology and pathogenesis,” *Thorax*, vol. 62, no. 4, pp. 360–367, 2007.
- [20] B. Z. Schmidt, J. B. Haaf, T. Leal, and S. Noel, “Cystic fibrosis transmembrane conductance regulator modulators in cystic fibrosis: Current perspectives,” *Clin. Pharmacol. Adv. Appl.*, vol. 8, pp. 127–140, 2016.
- [21] G. A. Duncan *et al.*, “Microstructural alterations of sputum in cystic fibrosis lung disease,” *JCI Insight*, vol. 1, no. 18, pp. 1–12, 2016.
- [22] P. M. Quinton, “Cystic fibrosis: impaired bicarbonate secretion and mucoviscidosis,” *Lancet*, vol. 372, no. 9636, pp. 415–417, 2008.
- [23] C. S. Rogers *et al.*, “The porcine lung as a potential model for cystic fibrosis,” *Am. J. Physiol. Cell. Mol. Physiol.*, vol. 295, no. 2, pp. L240–L263, 2008.
- [24] J. L. and J. L. P. Matthews, Leroyw, Spector Samuel, “Studies on pulmonary secretions,” pp. 83–87, 1963.
- [25] R. C. Boucher, “Cystic fibrosis: a disease of vulnerability to airway surface dehydration,” *Trends Mol. Med.*, vol. 13, no. 6, pp. 231–240, 2007.
- [26] J. V. Fahy, K. W. Kim, J. Liu, and H. A. Boushey, “Prominent neutrophilic inflammation in sputum from subjects with asthma exacerbation,” *J. Allergy Clin. Immunol.*, vol. 95, no. 4, pp. 843–852, 2005.
- [27] P. B. Davis, “Cystic fibrosis since 1938,” *Am. J. Respir. Crit. Care Med.*, vol. 173, no. 5, pp. 475–482, 2006.
- [28] L. P. Shulman and S. Elias, “Cystic Fibrosis,” *Clin. Perinatol.*, vol. 28, no. 2, pp. 383–393, 2001.
- [29] H. Matsui *et al.*, “A physical linkage between cystic fibrosis airway surface dehydration and *Pseudomonas aeruginosa* biofilms,” vol. 103, no. 48, 2006.
- [30] H. Matsui *et al.*, “Reduced Three-Dimensional Motility in Dehydrated Airway Mucus Prevents Neutrophil Capture and Killing Bacteria on Airway Epithelial Surfaces,” 2019.

- [31] J. S. Suk *et al.*, “The penetration of fresh undiluted sputum expectorated by cystic fibrosis patients by non-adhesive polymer nanoparticles,” *Biomaterials*, vol. 30, no. 13, pp. 2591–2597, 2009.
- [32] B. S. Schuster, J. Soo, G. F. Woodworth, and J. Hanes, “Biomaterials Nanoparticle diffusion in respiratory mucus from humans without lung disease,” *Biomaterials*, vol. 34, no. 13, pp. 3439–3446, 2013.
- [33] S. J.S., L. S.K., B. N.J., D. M.R., B. M.P., and H. J., “Rapid transport of muco-inert nanoparticles in cystic fibrosis sputum treated with N-acetyl cysteine,” *Nanomedicine*, vol. 6, no. 2, pp. 365–375, 2011.
- [34] B. S. Schuster *et al.*, “Overcoming the Cystic Fibrosis Sputum Barrier to Leading Adeno-associated Virus Gene Therapy Vectors,” *Mol. Ther.*, vol. 22, no. 8, pp. 1484–1493, 2014.
- [35] T. G. Mason, “Rheol Acta 2000 Mason,” pp. 1–8, 2000.
- [36] Y. Tsuji, X. Li, and M. Shibayama, “Evaluation of Mesh Size in Model Polymer Networks Consisting of Tetra-Arm and Linear Poly(ethylene glycol)s,” *Gels*, vol. 4, no. 2, p. 50, 2018.
- [37] L. Cai, S. Panyukov, and M. Rubinstein, “Mobility of Nonsticky Nanoparticles in Polymer Liquids,” pp. 7853–7863, 2011.
- [38] T. G. Mason, K. Ganesan, J. H. Van Zanten, D. Wirtz, and S. C. Kuo, “Particle Tracking Microrheology of Complex Fluids,” 1997.
- [39] S. Yuan *et al.*, “Oxidation increases mucin polymer cross-links to stiffen airway mucus gels,” *Sci. Transl. Med.*, vol. 7, no. 276, pp. 1–10, 2015.
- [40] J. A. Burns, J. C. Butler, J. Moran, and G. M. Whitesides, “Selective Reduction of Disulfides by Tris(2-carboxyethyl)phosphine,” *J. Org. Chem.*, vol. 56, no. 8, pp. 2648–2650, 1991.
- [41] S. Honda, Y. Matsuda, M. Takahashi, K. Kakehi, and S. Ganno, “Fluorimetric Determination of Reducing Carbohydrates with 2-Cyanoacetamide and Application to Automated Analysis of Carbohydrates as Borate Complexes,” *Anal. Chem.*, vol. 52, no. 7, pp. 1079–1082, 1980.
- [42] S. K. Lai, Y. Y. Wang, and J. Hanes, “Mucus-penetrating nanoparticles for drug and gene delivery to mucosal tissues,” *Adv. Drug Deliv. Rev.*, vol. 61, no. 2, pp. 158–171, 2009.
- [43] B. C. Tang *et al.*, “Biodegradable polymer nanoparticles that rapidly penetrate the human mucus barrier,” *Proc. Natl. Acad. Sci.*, vol. 106, no. 46, pp. 19268–19273, 2009.
- [44] M. N. Hurley, A. P. Prayle, and P. Flume, “Intravenous antibiotics for pulmonary exacerbations in people with cystic fibrosis,” *Cochrane Database Syst. Rev.*, vol. 2017, no. 6, 2015.
- [45] Saverio E. Spagnolie, “Complex Fluids in Biological Systems,” Nov 27, 2014.

Curriculum Vitae

Miss Wang Xiaoxin

Email: xiaoxinw@hotmail.com, Tel: +1- 4107109697

EDUCATION

Johns Hopkins University	Baltimore, Maryland
<i>Master of Science in Engineering(expected)</i>	08/2017-05/2019
Major: Chemical and Biomolecular Engineering	GPA: 3.78/4.0
Thesis Title: Developing Artificial Mucus Hydrogel that Mimics Cystic Fibrosis Airway Mucus	
East China Normal University	Shanghai, China
<i>Bachelor of Science</i>	09/2013-06/2017
Major: Chemistry	GPA:3.34/4.0
	Major GPA:3.5/4.0

RESEARCH EXPERIENCES

The Effect of Cystic Fibrosis (CF) Sputum's Microstructure on Bacteria Colonization and Neutrophil Migration

2/2018-Present

- Developed the permanent and bio-reducible artificial mucus hydrogel to mimic the microstructure of CF patients' sputum using mucin from porcine stomach (PGM) and crosslinkers
- Engineered mucus-penetrating nanoparticles (MPP) by coating the fluorescent beads with PEG at high densities required to make particle surfaces resistant to muco-adhesion
- Used MPP and conventional mucoadhesive nanoparticles (CP) as the probes, and performed fluorescent video microscopy experiments to track the motion of nanoparticles in models to evaluate the microstructure (MSD) of artificial mucus models and compared with CF sputum samples
- Evaluated the biochemicals (mucin, cysteines) concentration of artificial mucus hydrogel and compared with these of CF sputum samples
- Investigated the effect of mucolytics on artificial mucus hydrogel and compared its responsibility with that of CF sputum samples
- Determined the effect of microstructure of mucus hydrogel on bacteria colonization by evaluating the bacteria growth and microcolony development of bacteria in mucus hydrogel with different microstructures, and tend to prove that microcolonies are greater in mucus hydrogel with smaller pore size
- To determine the effect of microstructure of mucus on neutrophil migration by examining the neutrophil chemotaxis in gravitational and antigravitational directions in mucus hydrogel with different microstructures, and tend to prove that neutrophil migration will be hindered in mucus hydrogel with smaller pore size

- To determine the effect of microstructure of mucus on neutrophil-bacteria capture by investigating the survival of bacteria incubated with neutrophils in mucus hydrogel with different microstructures.

Microstructural Changes in CF Sputum Correlate with Patient Lung Function over Longitudinal Time Points

09/2017-Present

- Engineered mucus-penetrating particles (MPP) using fluorescent beads with controlled particle diameters densely coated with PEG to make particle surfaces resistant to muco-adhesion
- Compared those particles' physicochemical properties with non-pegylated counterparts (which is called conventional particles (CP) in this study), and proved MPP were muco-inert, stable and non-adhesive to CF sputum
- Quantified mucus solids content and measured the concentrations of mucin, DNA and cross-linked cysteine via well-established fluorometric assays, which led to the findings that individual sputum constituents collectively impacted on the microstructure of airway mucus
- Correlated biophysical (i.e. mucus microstructure or MSD) and biochemical (i.e. solids content and concentration of cross-linked cysteine) properties of sputum samples with lung functions of CF patients, which were measured by spirometry (i.e. FEV_{1s}) at the day of their clinical visit and sputum expectoration, and observed the trend of positive or negative correlations between FEV_{1s} and MSD or solids content
- Carried out a pilot longitudinal study to monitor the changes in sputum biophysical property (i.e. pore sizes or MSD) over subsequent clinical visits of CF patients, correlated the changes with their lung function changes, and concluded that our biophysical analysis of expectorated sputum may serve as a surrogate to monitor lung functions of CF patients over time
- Examined the utility of MSD measurements for evaluating the efficacies and kinetics of mucus-altering therapeutic agents via a pilot study, and proved that treatment of sputum with TCEP could significantly increase the pore sizes at a final concentration of 5 mM
- To investigate whether biophysical property, or perhaps biochemical properties, may provide a means to predict future exacerbation events among CF patients

A Biochemical Analysis of Chronic Obstructive Pulmonary Disease (COPD) Sputum Samples for Determination of Predictive Factors

10/2017-10/2018

- Analyzed features (biophysical and biochemical properties of the COPD sputum) including MSD, mucin solid concentration, mucin concentration, DNA concentration, disulfide bond concentration, Neutrophils (%), Macrophages (%) and Lymphocytes (%) to examine variation and correlation of the data. And correlated to patients' demographics.
- Correlated biophysical (i.e. mucus microstructure or MSD) and biochemical (i.e. solids content, osmotic pressure and concentration of cross-linked cysteine) properties of sputum samples with lung functions of COPD patients, which were measured by spirometry (i.e. FEV_{1s}) at the day of their clinical visit and sputum

expectoration, and observed the trend of positive or negative correlations between FEV_{1s} and MSD or solids content

- Examined the correlation between MSD and mucus solids, mucin content, DNA content and osmotic pressure and observed that there are obvious negative correlations with MSD and solids, osmotic pressure
- The first and second principal components of the PCA suggest its best to select Mucus solids, DNA concentration and Mucin concentration as inputs for a ML model for classification of COPD exacerbation.

Study about the Effect of Coated Protein Nanocages in Brain-Penetration and Doxorubicin Efficacy for Treatment of Aggressive Gliomas **01/2018-10/2018**

- Tested the moving ability (MSD; an averaged square of distance travelled by an individual particle over a given time interval) of Ftn-CY3 and PEG-Ftn-CY3 particles in normal and tumor brain section.
- The result shows that moving ability of Ftn-CY3 particles are increased with PEG coated, and the MSD value of Ftn-CY3 and PEG-Ftn-CY3 particles in tumor brain section is increased compared with normal brain section.

Synthesis and Characterization of Metal-fiber Structured Cu-Zn-Al Hydrotalcite-like Compounds

02/2017-

06/2017

- Combined merits of Layered Double Hydroxide (LDHs) and structured-supports together to develop metal-fiber structured Cu-Zn-Al-LDHs/FeCrAl-fiber, which has strong capacity to enhance mass/heat transfer and optimize fluid dynamics via in-situ hydrothermal growth method
- Optimized the preparation conditions of metal-fiber structured Cu-Zn-Al-LDHs/FeCrAl-fiber via adjusting support, pH value of solution, reaction temperature and reaction time

Study of the Applications for Determination of Polyamines Based on Capillary Electrophoresis Combined with Electromembrane Extraction

09/2015-05/2016

- A capillary electrophoresis with capacitively coupled contactless conductivity detection (CE-C4D) method was developed for direct determination of polyamines, and the detection sensitivity was significantly improved based on electromembrane extraction (EME)
- Ethanediamine and hexamethyldiamine are two diamine plastic restricted substances commonly existing in food contact materials and could be well separated from their aliphatic diamine homologs as well as the common inorganic cations within 25 min.
- Under the optimum conditions, the highest enrichment factor of ethanediamine and hexamethyldiamine were 718-fold and 660-fold, respectively, and the limits of detection were both 0.04 ng/mL.
- The research paper was published in the journal of Food Chemistry
- (IF 4.052, <http://dx.doi.org/10.1016/j.foodchem.2016.11.084>)

Catalysts Experiments

07/2016-08/2016

- The research work focused on the introduction of the second metal to modify the performance of Pd catalyst. The Pd-In (indium) bimetallic catalysts with different ratio of Pd/In, i.e. Pd₁In_{0.2}, Pd₁In_{0.4} and Pd₁In_{0.6} (where 1 and 0.6 represent the weight fraction of Pd and In in catalyst), were prepared with co-impregnation method.
- The results suggest that the insertion of In component can isolate Pd active sites, i.e., geometric interaction, which reduces acetylene adsorbed on Pd-In bimetallic surface in bridged forms and leads to weakly π -bonded acetylene on top sites of isolated Pd.

SKILLS

- Computer Skills: Python, Origin, Matlab, Graphpad
- Experimental skills: Nanoparticle Modification, Drugs Modification, Polymer Conjugation, Fluorescent Video Microscopy Experiment, Cell Culture, Bacteria Culture, Bacteria Transformation, Neutrophil Isolation, Animal Experiment and Surgery.
- Languages: Chinese and English